PLANETARY SCIENCE

Complex organosulfur molecules on comet 67P: Evidence from the ROSINA measurements and insights from laboratory simulations

Ahmed Mahjoub[1,2]*, Kathrin Altwegg[3], Michael J. Poston[4], Martin Rubin[3], Robert Hodyss[1], Mathieu Choukroun[1], Bethany L. Ehlmann[5], Nora Hänni[3], Michael E. Brown[5], Jordana Blacksberg[1], John M. Eiler[5], Kevin P. Hand[1]

The ROSINA (Rosetta Orbiter Spectrometer for Ion and Neutral Analysis) instrument aboard the Rosetta mission revolutionized our understanding of cometary material composition. One of Rosetta's key findings is the complexity of the composition of comet 67P/Churyumov-Gerasimenko. Here, we used ROSINA data to analyze dust particles that were volatilized during a dust event in September 2016 and report the detection of large organosulfur species and an increase in the abundances of sulfurous species previously detected in the coma. Our data support the presence of complex sulfur-bearing organics on the surface of the comet. In addition, we conducted laboratory simulations that show that this material may have formed from chemical reactions that were initiated by the irradiation of mixed ices containing H_2S. Our findings highlight the importance of sulfur chemistry in cometary and precometary materials and the possibility of characterizing organosulfur materials in other comets and small icy bodies using the James Webb Space Telescope.

INTRODUCTION

The Rosetta mission's visit to the comet 67P revealed a remarkable diversity of organic molecules in the comet's materials (*1*). During the Rosetta mission, organics were detected by the remote sensing instrument VIRTIS (Visible and Infrared Thermal Imaging Spectrometer) (*2*) as well as in situ instruments, including ROSINA (Rosetta Orbiter Spectrometer for Ion and Neutral Analysis) (*3*), Ptolemy (*4*), and COSAC (Cometary Sampling and Composition experiment) (*5*). ROSINA measurements substantially improved our understanding of the complex organic chemistry in the cometary materials, and ROSINA measurements during enhanced dust emission events offered insights into the composition of the semivolatile phases of the comet 67P. These phases can be regarded as a bridge between the gas phase composition of the comet coma and the nonvolatile refractory organics. Measurements from such events have already proven to be very informative, leading to the detection of complex organic molecules (*6*), the detection of ammonium salts (*7*), and, more recently, the detection of high abundance of ammonium hydrosulfide salt NH_4^+ SH^- (*8*).

Reactions on the surfaces of icy grains are believed to play a pivotal role in the chemistry of dense molecular clouds and solar nebulae (*9*). These reactions are mainly initiated by ultraviolet (UV) photons (either external or from the young star) or by bombardment by energetic particles. Hence, analysis of the cometary materials could enhance our understanding of this grain-surface photo- and radiolytic chemistry. Laboratory simulations of this chemical processing are needed to decipher the link between cometary molecules detected by Rosetta and the reservoirs from which comets are formed. Growing evidence suggests that H_2S was a highly abundant molecule in the presolar nebula (*8*, *10*). The Rosetta mission to comet 67P demonstrated that H_2S is the fifth most abundant molecule in the coma after H_2O, CO, CO_2, and O_2 (*10*). A recently published analysis of ROSINA-DFMS (Double Focusing Mass Spectrometer) data during multiple dust events shows a very high abundance of NH_3 and H_2S, believed to result from the decomposition of ammonium hydrosulfide (*8*). During some of these dust events, H_2S and NH_3 were more abundant than even water (*8*). Despite the importance of H_2S and the potential of sulfur chemistry to considerably affect the chemical reactivity in mixed ices, little has been published exploring this chemistry. We recently demonstrated that H_2S could markedly affect the chemistry (*11*, *12*) and spectroscopy (*13*, *14*) of mixed ices relevant to small icy bodies—particularly Kuiper belt objects (KBOs) and Jupiter Trojans (*15*). Sulfur chemistry could also play an important role in prebiotic chemistry and abiotic synthesis of biomolecules such as amino acids (*16*).

Here, we discuss data from Rosetta/ROSINA measurements obtained during an event of enhanced dust impacts into the instrument and interpret these data as showing the presence of large organosulfur molecules with low volatility embedded in the dust grains in comet 67P. We also report laboratory simulations of organic chemistry initiated by irradiation of simple ice mixtures with and without H_2S. This laboratory work shows that sulfur dominates the chemistry when H_2S is included and points toward a possible ice-chemistry origin of the diversity of sulfur-bearing species detected in the cometary material.

[1]Jet Propulsion Laboratory, California Institute of Technology, Pasadena, CA 91109, USA. [2]Space Science Institute, 4765 Walnut St, Suite B, Boulder, CO 80301, USA. [3]Physikalisches Institut, University of Bern, Bern, Switzerland. [4]SWRI, San Antonio, TX 78238, USA. [5]Division of Planetary and Space Sciences, Caltech, Pasadena, CA 91125, USA.
*Corresponding author. Email: amahjoub@spacescience.org

RESULTS

The dust event

In the last few weeks of the mission before landing on the comet, Rosetta flew elliptical orbits with the pericenter altitude gradually

lowered (and the apocenter altitude increased, keeping the size of the ellipse constant). On 5 September 2016, around 22:00 UTC, the spacecraft reached its closest distance from the comet, 3.9 km from the comet center (approximately 1.9 km above the surface). Shortly before that, Rosetta was most probably hit by a chunk of ice and dust, showing high-density gas peaks for more than 3 hours in the vicinity of the ROSINA-COPS [COmetary Pressure Sensor; more details about ROSINA instruments can be found in the study by Balsiger *et al.* (*17*)] nude gauge with its field of view of 340°. Around 19:00 UTC, the nude gauge was saturated. The COPS ram gauge, measuring ram pressure and pointing toward the comet, showed large pressure spikes around 18:00 UTC, most likely dust-ice grains entering the equilibrium chamber and sublimating inside the gauge. The ROSINA-DFMS also registered the event. The data from the ROSINA-COPS were very reproducible, suggesting very stable outgassing before the dust event took place around 18:00 UTC. During the event, the total density, as measured by ROSINA-COPS, increased by about one order of magnitude; shortly after 20:00 UTC, the density returned to normal values. More details about the dust event are given in the references (*7*, *18*).

ROSINA measurements of sulfur-rich organics

Figure 1 shows the abundances of various sulfur-bearing molecules before and after the dust event. Samples of mass spectra from which these abundances were determined are given in the Supplementary Materials (figs. S2 to S6). Abundances are given in arbitrary units but corrected for instrumental effects (mass-dependent sensitivity). The ROSINA-DFMS instrument had previously detected multiple sulfurous molecules in the undisturbed coma of comet 67P, as reported by Calmonte *et al.* (*19*); ROSINA's high mass resolution enabled precise molecular assignments. However, during the dust event (on 5 September 2016), ROSINA-DFMS measured an increase by a factor between 10 and 100 for many of these molecules, compared to the abundance just before the event around 17:00. S_2, S_3, and H_2S increased in abundance by a factor of 100, 10, and 100, respectively. Sulfur dioxide (SO_2) also increased by about two orders of magnitude. SO has an abundance during the event comparable to that of SO_2; however, its abundance right before the event could not be determined because of corruption of the spectrum. Carbonyl sulfide (COS) and carbon disulfide (CS_2) are the only species that did not increase during the dust event. These molecules are much more volatile than the other S species considered here, which could explain the depletion of these two molecules.

Hereafter, we focus on the plethora of sulfurous molecules that are not detected in the undisturbed coma but detected by the ROSINA-DFMS instrument during the dust event that establish the presence of semivolatile organo-sulfurous molecules on the surface of comet 67P. These are mainly heavy molecules (or fragments due to dissociation of larger molecules) that are not volatile enough to be detected in the gas phase. Their detectability was enhanced during the dust event because of volatilization upon impact with the Rosetta spacecraft and sublimation inside ROSINA, which was warmer than the comet. During the dust event, particles entered the instrument's ion source at 273 K (*18*). Semivolatile molecules

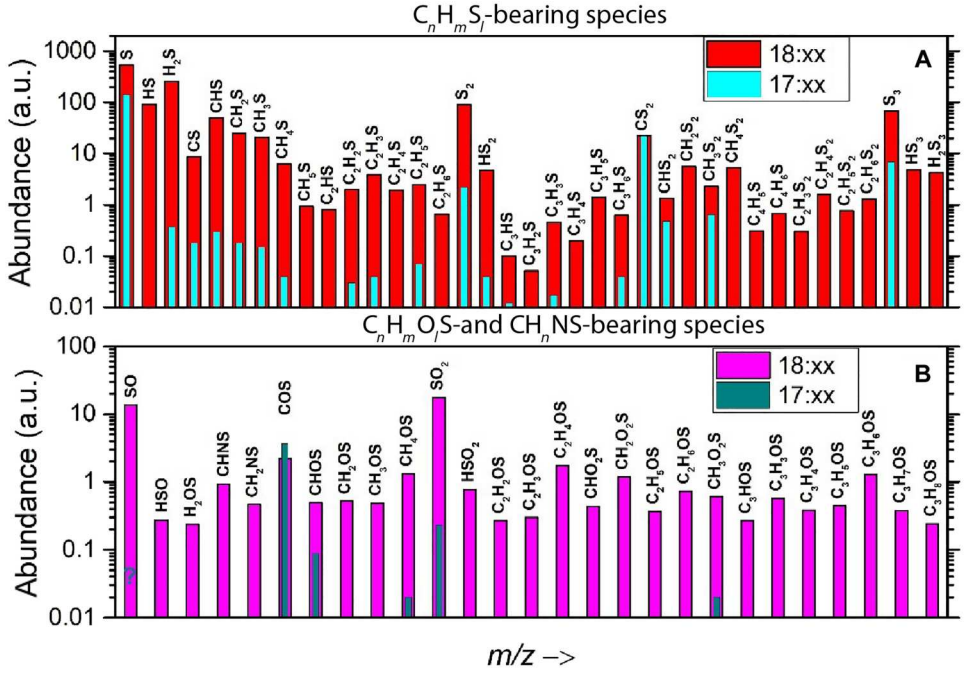

Fig. 1. Sulfur-bearing species detected by ROSINA (Rosetta Orbiter Spectrometer for Ion and Neutral Analysis)–DFMS (Double Focusing Mass Spectrometer) before and during the dust event on 5 September 2016, ~2 km above the nucleus surface. 17:xx denotes measurements made before the dust impact between 17:15 and 17:55 UTC (depending on mass), and 18:xx denotes measurements during the dust impact (18:09 to 18:50). (**A**) $C_nH_mS_l$ bearing species, $n = 0$ to 4; $m = 0$ to 6, $l = 1$ to 2. (**B**) $C_nH_mO_lS$- and CH_nNS-bearing species, $n = 0$ to 3; $m = 0$ to 6, $l = 1$ to 2. Species are ordered by mass/charge ratio (m/z) but not spaced accordingly (x axis not linear). The value, pre-event, for SO could not be derived as the spectrum is corrupted. Abundances are given in arbitrary units (a.u.) but corrected for instrumental effects (mass-dependent sensitivity). Caution: During the impact, coma background densities decreased over the 40 min needed to cover the mass range. Higher masses are therefore underestimated compared to low masses.

sublimated slowly over the course of many hours at this temperature.

Detected S-bearing species can be categorized into three families: $C_nH_mS_l$-bearing molecules with elemental abundances (n = 0 to 4; m = 0 to 6, l = 1 and 2), $C_nH_mO_lS$ (n = 0 to 3; m = 0 to 6, l = 1 to 2) and CH_nNS (n = 1 to 2). Among the $C_nH_mS_l$ family, only CH_4S and C_2H_6S had previously been detected in the coma (*19*). During the dust event, more complex species with up to four carbon atoms were identified. For n = 1 (one carbon atom) detected species are CS, CHS, CH_2S, CH_3S, CH_4S, and CH_5S. CH_4S had previously been detected in the coma and was assigned as methanethiol (CH_3SH) because the fragments and protonated species expected from impact ionization (CH_3S and CH_3SH_2) were also detected. CH_2S could be assigned to thioformaldehyde, which could exist in the cometary material as a monomer or as a result of dissociation of a larger polymer (thioformaldehyde is known to be unstable at room temperature and to quickly polymerize). This interpretation is supported by the detection of the thioformaldehyde dimer ($2•CH_2S$) in the n = 2 family (see Fig. 1).

For $C_nH_mS_l$ with n and/or l greater than 1, species containing up to four carbon atoms were observed with notable abundances, while in the undisturbed coma, only $C_2H_6S_2$ was observed. These species could be products of dissociation of larger polymers that are not stable at T = 273 K, and some of them could also be products of fragmentation by electron impact inside the mass spectrometer. For the family $C_nH_mO_lS$, only COS has been detected in the undisturbed coma. During the dust event, multiple species were detected within this family. Most of these species contain only one oxygen atom (C_nH_mOS) with up to three carbon atoms. These species resemble hydrocarbons substituted with an OS group. Each of these species could correspond to a large variety of isomers, and their fragmentation patterns are complex; therefore, it is hard to disentangle the parent molecules from the daughter species produced by dissociative reactions. Another important result from the ROSINA data is the detection of CH_nNS in the coma of comet 67P. While NS was tentatively detected by Calmonte *et al.* (*19*), CHNS and CH_2NS are the first species containing C, N, and S atoms to be detected.

Laboratory simulations

The ROSINA-DFMS data recorded during the dust event and presented above indicate a sulfur chemistry more complex and diverse than previously anticipated from the measurements in the undisturbed coma (*19*). The variety of sulfur-bearing molecules detected in the cometary material by the ROSINA instrument is believed to be a result of ice chemistry involving H_2S (*20*). To investigate the effect of H_2S on this chemistry, we performed electron irradiation experiments on ice mixtures with and without H_2S. Details about the protocols and apparatus used for this laboratory simulation are summarized in Materials and Methods below. Briefly, the setup is a high-vacuum stainless steel chamber that reaches a pressure of approximately 1×10^{-8} torr. The ices were deposited on a gold substrate attached to the cold finger of a helium cryostat using a gas manifold to prepare gas mixtures. An electron gun was mounted on the chamber perpendicular to the substrate, and a Faraday cup was used to monitor the electron beam current. The chemical evolution of the samples was monitored using a Fourier transform infrared (FTIR) spectrometer.

Two ice samples "without sulfur" $CH_3OH:NH_3:H_2O$ (3:3:1) and "with sulfur" $CH_3OH:NH_3:H_2S:H_2O$ (3:3:3:1) were deposited under vacuum at T = 50 K and irradiated with a 10-keV electron gun. Both samples were irradiated for 20 hours with a beam current of 0.5 μA corresponding to a total fluence of electron energy $\sim 2 \times 10^{21}$ eV cm^{-2}. After irradiation, both samples were warmed up to 120 K at a rate of 0.5 K min^{-1} and held there for one additional hour under continued electron irradiation. Both samples were then warmed to room temperature at a rate of 0.5 K min^{-1}. The gases sublimating from the irradiated ices were detected with a Stanford Research System RGA (Residual Gas Analyzer) 200 quadrupole mass spectrometer, operated with 70-eV electron impact ionization and mass resolution <0.5 amu. The refractory thin films remaining after warming to room temperature were characterized by infrared (IR) spectroscopy. The ice mixtures presented here are depleted in water compared to the composition of comets and protoplanetary disks and interstellar ices. This was necessary to increase the detectability of minor irradiation products that would otherwise be hard to detect at very low abundances. A separate test was conducted with a more representative mixture of $CH_3OH:NH_3:H_2S:H_2O$ (10:1:1:100), and the results presented and discussed in the Supplementary Materials.

Our laboratory simulations investigate the sulfur chemistry triggered by energetic processing of ice grains in the presolar nebula. According to Ciesla and Sandford (*21*), these grains are exposed to temperatures ranging from 30 K to approximately 120 K, based on their dynamical evolution. We conducted our irradiation experiment under temperatures within this range. Our working pressure is also relevant to the outer solar nebula, estimated to be $<10^{-6}$ bar (*22*). To initiate the radiolytic chemistry, we used 10-keV electrons. At this electron energy, the penetration depth is approximately 2.6 μm (into water ice), which is close to the thickness of our ice films (~2 μm) and ensures that most of the beam energy is deposited in the film. The total fluence received by irradiated samples is $\sim 2 \times 10^{21}$ eV cm^{-2}, corresponding to a dose of 600 eV/16 amu. This irradiation dose is scalable to an irradiation time in the presolar nebula between 3.7 and 37 million years (Ma) (see details in Materials and Methods). It is worth noting that UV (*23*), x-ray (*24*), and ion (*25*) irradiations, among other sources, likely played a role in the processing of icy grains in the presolar nebula. We intend to carry out further studies to compare the impact of different energy sources on the sulfur chemistry.

Figure 2 shows a comparison between the mass spectra at T = 275 K of species desorbed from the "with sulfur" and the "without sulfur" irradiated ices. The two spectra are quite different especially at high mass/charge ratio (m/z), indicating the important role of sulfur chemistry. The spectrum of the "with sulfur" sample displays multiple additional peaks clearly undetected in the sample "without sulfur." This implies that these species are sulfur-bearing molecules. These additional peaks dominate the mass spectrum of the "with sulfur" sample, indicating a very rich sulfur chemistry. This was confirmed by IR spectroscopy of the residues left at room temperature, as discussed later. Note that the mass resolution of our mass spectrometer is much lower than the ROSINA-DFMS instrument and could not resolve the different species that might contribute to the signal at each m/z. The assignment of peaks displayed in Fig. 2 is limited to species confirmed by IR spectroscopy (*11*) or by Temperature Programmed Desorption (TPD) verification of fragmentation patterns (*12*).

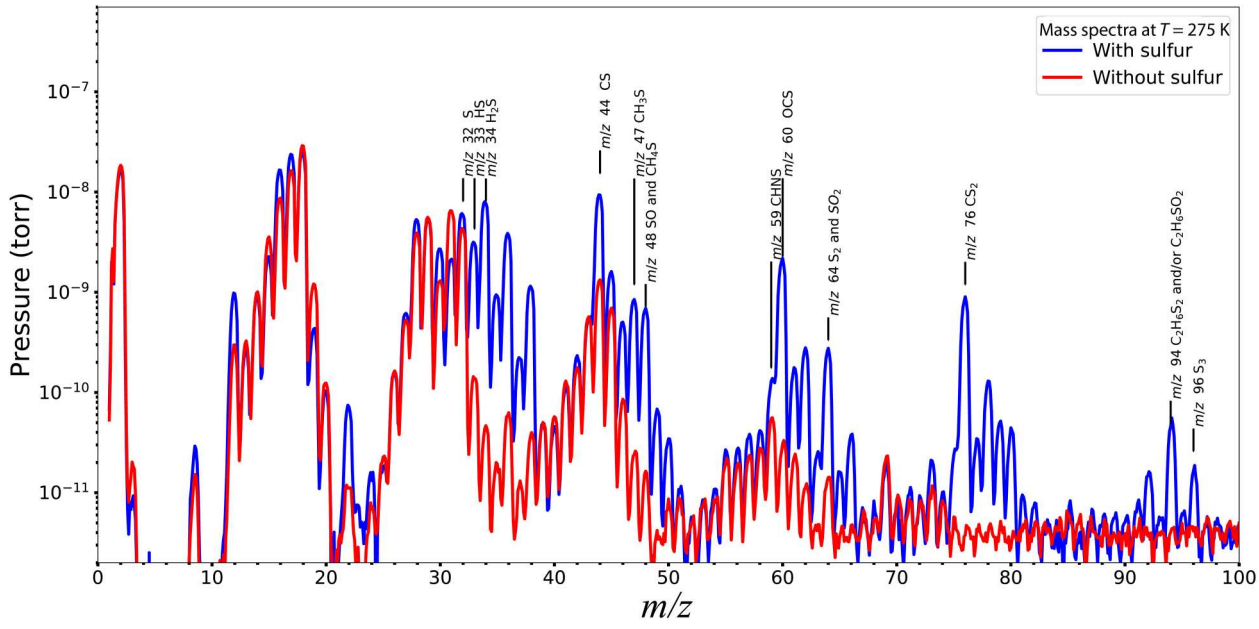

Fig. 2. Comparison between mass spectra of species desorbed from "with sulfur" (blue) and "without sulfur" (red) irradiated ice mixtures in the laboratory experiments. Both spectra are recorded at $T = 275$ K, and both samples received similar irradiation doses. *m/z*, mass/charge ratio.

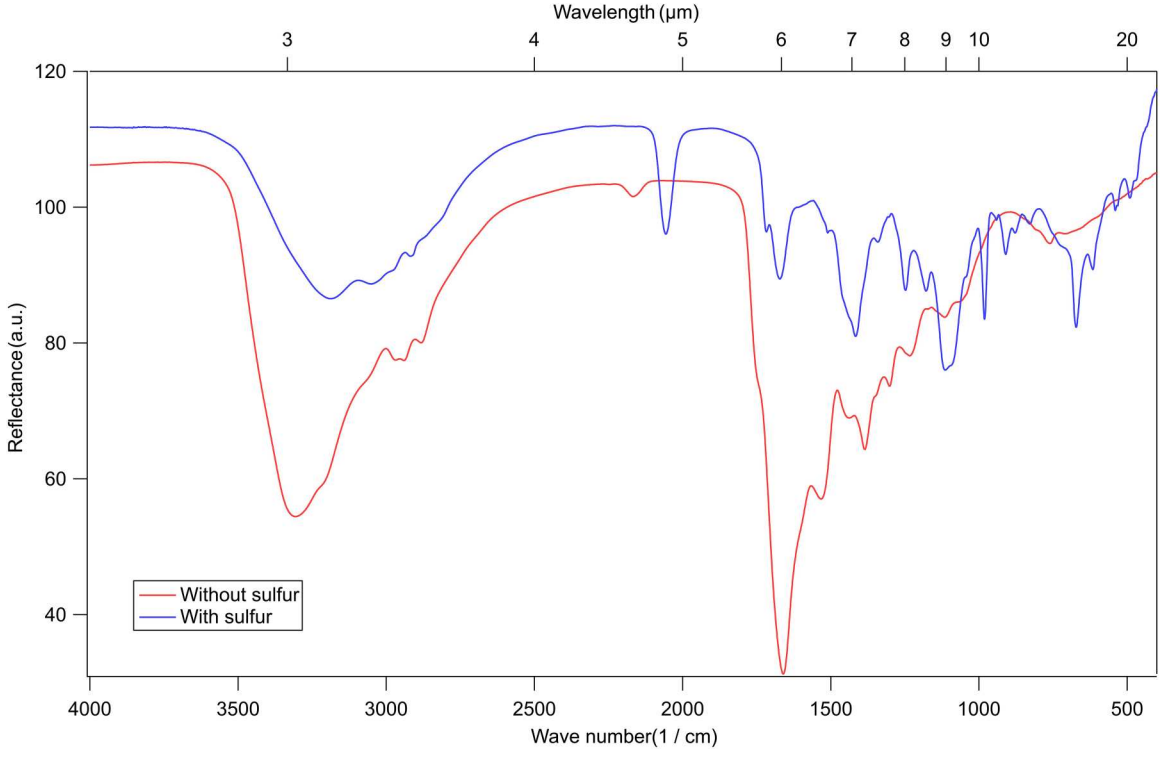

Fig. 3. Comparison between the infrared (IR) spectra of "without sulfur" residue (red spectrum) and "with sulfur" residue samples (blue spectrum). Both samples were produced by irradiating ice films with a 10-keV electron beam for 20 hours at 50 K. This irradiation time is equivalent to a total fluence of 2×10^{21} eV cm^{-2}. Initial ices are made of CH_3OH:NH_3:H_2S:H_2O (3:3:3:1) ("with sulfur") and CH_3OH:NH_3:H_2O (3:3:1) ("without sulfur"). a.u., arbitrary units.

Table 1. List of sulfur-bearing species detected by ROSINA (Rosetta Orbiter Spectrometer for Ion and Neutral Analysis)–DFMS (Double Focusing Mass Spectrometer) instrument with abundance > 1 arbitrary units (a.u.) compared to detections in mass spectra from the laboratory experiment. Because of the fragmentation inside the ROSINA-DFMS instrument, many of the species detected could be fragments of larger parent molecules (see discussion in the ROSINA data paragraph). *m/z*, mass/charge ratio

Detection by ROSINA (abundance >1 a.u.)	Detection in laboratory	Detection by ROSINA (abundance >1 a.u.)	Detection in laboratory
CS (*m/z* 44)	Confirmed by IR	CH_2S_2 (*m/z* 78)	Assignment cannot be confirmed
CSH (*m/z* 45)	Assignment cannot be confirmed	CH_4S_2 (*m/z* 80)	Assignment cannot be confirmed
CH_2S (*m/z* 46)	Assignment cannot be confirmed	$C_2H_6S_2$ (*m/z* 94)	Confirmed by TPD
CH_3S (*m/z* 47)	Confirmed by fragment patterns	S_3 (*m/z* 96)	Confirmed by TPD
CH_4S (*m/z* 48)	Confirmed by fragment patterns	SO (*m/z* 48)	Confirmed by IR
C_2H_2S (*m/z* 58)	Assignment cannot be confirmed	CHNS (*m/z* 59)	Confirmed by comparison with NIST data
C_2H_3S (*m/z* 59)	Assignment cannot be confirmed	COS (*m/z* 60)	Confirmed by IR
C_2H_4S (*m/z* 60)	Assignment cannot be confirmed	CH_4OS (*m/z* 64)	Assignment cannot be confirmed
C_2H_5S (*m/z* 61)	Assignment cannot be confirmed	SO_2 (*m/z* 64)	Confirmed by IR
S_2 (*m/z* 64)	Confirmed by TPD	C_2H_4OS (*m/z* 61)	Assignment cannot be confirmed
C_3H_5S (*m/z* 73)	Assignment cannot be confirmed	CH_2O_2S (*m/z* 78)	Assignment cannot be confirmed
CS_2 (*m/z* 76)	Confirmed by IR	C_3H_6OS (*m/z* 90)	Assignment cannot be confirmed
CHS_2 (*m/z* 77)	Assignment cannot be confirmed		

We focus our comparison of the mass spectra between the ROSINA data and the laboratory measurements on S-bearing species with an abundance >1 a.u. ($\sim^1/_{200}$ the abundance of H_2S) (Table 1). For all these species, a peak was observed in the mass spectrum of the laboratory "with sulfur" sample, but the assignment could not be confirmed for all of them. In the Supplementary Materials, we discuss the possible contributors of each peak based on the National Institute of Standards and Technology (NIST) database for mass spectra of sulfur-bearing molecules. Many of the molecules, such as COS, SO_2, CS, and CS_2 (*11*), have previously been confirmed in the IR spectrum of the irradiated ice mixtures. Sulfur allotropes have also been confirmed by TPD measurements (*12*). Among the 25 species detected by ROSINA and listed in Table 1, we are able to confirm the production of 11 molecules in our laboratory simulation. The species C_2H_nS (n = 2 to 5) are probably fragments of $C_2H_6S_2$ that was previously detected, and it is likely that these species contributed to the mass spectrum, but we cannot confirm the detection of these species. Although we cannot firmly confirm the production of all sulfurous species detected by ROSINA, our laboratory work can reproduce the three families of S-bearing molecules found in comet 67P (see Fig. 1).

At room temperature, organic residues remained on the gold substrates for both samples. These organic refractory materials are proposed as analogs of the refractory organics in cometary materials. The COSIMA (COmetary Secondary Mass Analyzer) instrument has provided insight into the characterization of refractory organics in particles from comet 67P, revealing the detection of high–molecular weight organic matter (*26*). In addition, the detection of sulfur atoms (as well as possibly S_2 and S_3 allotropes) in these particles has also been confirmed by COSIMA (*27*). However, it has been challenging to determine the source of sulfur, as it could have been derived from either organics, minerals, or a combination of both. The semivolatile organics such the one detected by Hänni *et al.* (*6*) and the S-bearing molecules reported here are believed to be a link between the gas phase and the refractory organics in comet 67P as measured by COSIMA. Consequently, we also characterized the residues produced in our laboratory samples "with sulfur" and "without sulfur" using IR spectroscopy (Fig. 3; table S1 summarizes all bands observed in both samples with tentative assignments to particular vibrational modes).

Comparison between these two spectra shows a clear difference over the entire spectrum, suggesting a marked change in the chemical composition of the residue when H_2S participates in the reaction chemistry. The strong NH and OH bands at 3200 and 3300 cm^{-1} as well as the CN and CO bands around 1600 and 2200 cm^{-1} were clearly decreased in the "with sulfur" sample compared to the "without sulfur" sample; the same decrease is also observed for bands around 3000 cm^{-1}, assigned to CH stretching modes. For example, the C═O absorption band at 1660 cm^{-1} is three times deeper in the "without sulfur" sample, while the broad band between 3000 and 3200 cm^{-1} is two times deeper. The shape of this band around 3100 cm^{-1} is also different between the two samples, with the center shifted to higher wave numbers by 110 cm^{-1} in the "with sulfur" residue. The decrease of CO, CN, CH_x, NH_x, and OH strongly implies a depression of carbon-, nitrogen- and oxygen-containing compounds in the residue when H_2S is added to the ice composition.

A clear difference between the two spectra is the strong band at 2057 cm^{-1} in the "with sulfur" sample that is totally absent in the "without sulfur" sample. This band is correlated to sulfur and could be tentatively assigned to the N═C═S group. This band may be a good probe for the sulfur residue, although CO_3 also has a weak absorption feature at this wavelength. In the fingerprint region, the "with sulfur" residue displays strong bands between 500 and 700 cm^{-1} and between 1000 and 1500 cm^{-1}, which are not observed in the "without sulfur" sample. These absorption features are

assigned to sulfur containing CS, SO, and SS vibrational modes. A group of these features is compatible with polymers of CH_2S (thioformaldehyde): Bands at 670, 986, 1247, and 1446 cm^{-1} are compatible with the strongest bands of CH_2S dimer and trimer (*28*). Also, weak bands observed at 477 and 876 cm^{-1} are in good agreement with symmetric and asymmetric SS stretching modes in H_2S_x species as measured by IR spectroscopy for H_2S_3 and H_2S_4 (*29*). The vibrational modes SS and CS usually result in weak absorption bands below 900 cm^{-1} (*30*).

The magnitude of the observed bands in the spectrum of the "with sulfur" sample suggests that molecules/functional groups rich in sulfur dominate the composition of the residue "with sulfur." One hypothesis to explain the impact of H_2S on the chemistry of the ice samples is the difference in dissociation energies among H_2S, water, and methanol. The dissociation energy of the SH bond in H_2S [376.2 kJ/mol (*31*)] is substantially lower than those of the OH bond for water [492.6 kJ/mol (*31*)] or methanol (463 kJ/mol). The rapid dissociation of H_2S compared to methanol and water will produce a high concentration of radical HS and free sulfur atoms compared to the concentrations of OH and O produced by dissociation of water and methanol. These reactive sulfur-bearing radicals, present at high concentration quickly after the beginning of irradiation, will react with CO and CH_3 and CH_2 radicals produced by dissociation of methanol. This could affect the chemistry in the ice films and enhance the production of molecules rich in CS, OS and SS bonds.

DISCUSSIONS

These results show that the effect of H_2S on the refractory residue is important and should be considered in the characterization of organic heteropolymers in small icy bodies and interstellar icy grains. The similarity between the large, low-volatility sulfur-containing molecules detected in the 67P cometary dust grains and those produced in our laboratory experiments suggests that H_2S ice chemistry is likely responsible for the observed species. However, it is worth noting that other pathways could also contribute to the formation of organosulfur compounds in both the diffuse interstellar medium and the solar nebula. For instance, laboratory simulations have shown that a variety of sulfur-bearing organic compounds are formed by sulfur ion bombardment of astrophysical ices containing carbon, oxygen, and nitrogen sources (*32*, *33*). The residue from these experiments contained more than 9000 molecules, and 12% of them contain sulfur atoms. The range of masses detected in those studies is $m/z > 147$ Da, which preclude their comparison to the sulfurous species detected by ROSINA-DFMS during the dust event in the range $m/z < 100$ Da.

Our work supports the hypothesis that organosulfur residues could be an important reservoir for sulfur in molecular clouds (*23*). The abundance of gaseous sulfur in dense clouds and circumstellar regions is only a small fraction (0.3 to 0.1%) of its cosmic abundance, a discrepancy that is known as The Sulfur Depletion Puzzle (*34*, *35*), while in diffuse clouds, the sulfur abundance agrees with the cosmic abundance (*36*). The fact that sulfur-containing organic heteropolymers are not volatile means that they cannot be detected with ground-based submillimeter telescopic observations. While a paucity of production rates for sulfur residues have hindered evaluation of the S sink in the modeling of the hot molecular cores (*37*), the results from ion irradiation experiments (*25*), this work, and recent gas-grain astrochemical modeling (*37*) indicate that organosulfur molecules made of CNOH atoms mixed with S could be the main sink for sulfur in the dense clouds. We also suggest that organic sulfurous species should be considered in accounting for some of the 89 ± 8% of elemental sulfur in refractory form, estimated for disks from the accretion-contaminated photospheres of stars, in addition to a hypothesized sulfide mineral sink (*38*).

Tracing organosulfur molecules in meteoritic materials also points to a potential key role for H_2S ice. Recent samples returned by the Hayabusa-2 mission from asteroid Ryugu have revealed the presence of a wide range of sulfur-bearing species (*39*). Molecules containing CHS, CHOS, and CHONS functional groups have been detected in the soluble organic matter, and the estimated total sulfur bulk composition is approximately 3.3 weight %, corresponding to a C/S ratio of ~1.15. Organosulfur molecules have also been detected in the insoluble organic matter of Murchison and Allende meteorites, even though the chemistry creating these species is not known (*40*). A carbon-rich clast with exceptionally high sulfur was found in a carbonaceous chondrite meteorite and may have originated from a comet containing H_2S ice (*41*), and Vacher *et al.* (*42*) identified sulfur isotope anomalies in unique minerals within a primitive carbonaceous chondrite, which they hypothesized may have resulted from UV irradiation of H_2S ice in the solar nebula, subsequently incorporated into the parent asteroid of the meteorite.

The James Webb Space Telescope (JWST) is expected to substantially increase our understanding of the chemistry of the solar system (*43*) including comets (*44*), asteroids (*45*), and KBOs. The large wavelength coverage of 0.6 to 28.5 μm and the high sensitivity (10× to 100× that of current facilities) will help reveal the composition of a considerable number of small icy bodies and the similarities and differences between their compositions. This in turn will enable the evaluation of hypotheses about the formation and evolution of the solar system. Sulfur chemistry is particularly interesting in this context and could provide a rich source of knowledge about the formation and evolution of the solar system. For example, Wong and Brown (*46*) demonstrated that the sublimation line of H_2S is located within the belt of primordial planetesimals. Therefore, these objects would have been divided into two groups: those that retained H_2S for enough time to develop a sulfur-containing organic crust and those that did not. The clear effect of adding H_2S to the irradiation chemistry of mixed ices of simple molecules and the very pronounced difference between the spectra of "with sulfur" and "without sulfur" residue samples (Fig. 3) open an opportunity to distinguish H_2S retention in a wide range of small icy bodies. The high resolving power of the MIRI (Mid-infrared Instrument) of JWST ($2200 < \lambda/\Delta\lambda < 3500$) will enable detailed characterization of the surface composition. The NIRSpec (Near Infrared Spectrograph) instrument with its 0.6- to 5.0-μm spectral range and its high resolving power will provide access to measurements of the interesting 3.2-μm region as well as the 1.8-μm feature that is present only in the "with sulfur" sample (*14*). All these absorption features provide a fingerprint of the sulfur chemistry that make it highly discernable from other materials expected in comets and other small icy bodies surfaces such as water ice and minerals.

In conclusion, the fate of sulfur in the building blocks of the solar system and its incorporation into various small bodies is still not fully understood. However, it holds the potential to provide

answers regarding the origin and evolution of these small bodies and test the links between them.

MATERIALS AND METHODS

Laboratory simulations

Electron irradiation experiments were carried out in the Ocean Worlds Lab (http://oceanworldslab.jpl.nasa.gov). A detailed description of the facilities and the capabilities of this laboratory can be found in (*47*). The experimental setup consists of a high-vacuum stainless steel chamber pumped by a Varian Turbo pump and backed by oil-free pumps (pressure after overnight pumping about 1×10^{-8} torr). The ices were vapor-deposited on a substrate attached to the cold finger of a closed-cycle helium cryostat (ARS model DE-204). An attached gas manifold was used to prepare gas mixtures before deposition. The ice films were grown by leaking the gas mixture onto the mirror substrate at a controlled rate through capillary tubes just above the sample, forming ices on the substrate, which was held at 50 K. Two different ice mixtures are considered in this study, and they were made from two different gas mixtures: "without sulfur" CH_3OH:NH_3:H_2O (3:3:1) and "with sulfur" CH_3OH:NH_3:H_2S:H_2O (3:3:3:1). The composition of the ice films could be slightly different because of the different sticking efficiency of each type of molecule in the mixture.

High-energy electrons (10 keV) were directed at the ice with a typical beam current of 0.5 μA. All studied ices were subjected to the same fluence of electron energy $\sim 2 \times 10^{21}$ eV cm^{-2}. Radiation fluences were scaled to the outer solar system based on the electron flux at 1 au, which was deduced from values given by Bennett *et al.* (*48*). We found that the total fluence received by our ice samples corresponds to a time scale of 0.2 Ma for an object at 5 au and 1.8 Ma at 15 au. This energy could also be scaled to energy received by icy grains in presolar nebula using the cosmic ray flux as reported by Yeghikyan (*49*). We found an irradiation time between 3.7 and 37 Ma depending on the density of the nebula. The processes simulated here are processes in the presolar nebula.

After irradiation for 20 hours at 50 K, samples were warmed to 120 K at a rate of 0.5 K min^{-1} and held there for one additional hour under continued electron irradiation. After the electron irradiation was concluded, the samples were warmed at a rate of 0.5 K min^{-1} to 300 K. The resulting residue films were characterized at room temperature by specular reflectance spectroscopy, using an FTIR spectrometer.

ROSINA-DFMS data analysis

Details on data analysis methods for ROSINA-DFMS are given in (*3*, *19*). ROSINA-DFMS steps through integer masses with an integration time of 20 s per mass. The neutral molecules are ionized by 45-eV electrons, which leads to parent ions as well as fragment ions. The detector has two times 512 anodes, which register the incoming ions. The peak shape on the detector can be described very well by a double Gaussian, whereby the second Gaussian has a width about three times the width of the first one and the amplitude is <10% of the peak amplitude. For small peaks, the smaller Gaussian is often not seen. The width is not dependent on the location on the detector as long as it is relatively close to the center. This means that if we have several peaks, we can use the same width for all of them. Once species have been identified, we also know their exact masses. This allows the disentanglement of even several masses close together with high confidence. Figures S2 to S6 show five representative spectra for CHNS (m/z 59), C_3H_6S (m/z 62), S_2 (m/z 64), C_3H_6OS (m/z 78), and S_3 (m/z 96). Given are spectra from before the impact (blue) and after the impact (black). Because at that time, the pressure inside the ion source of ROSINA-DFMS was still changing rapidly, peak heights cannot easily be compared between masses. An example for the Gaussian fits is given in fig. S1 for m/z = 59 where we fit five masses, all with the same width. In this case, the second Gaussian is mostly unimportant as it affects only the tails of the peaks. From such fits, we obtain the peak heights and the peak areas. For the other spectra, we do not plot the fits for readability reasons. In the present analysis, we use peak height in arbitrary units and correct them for the mass (energy)–dependent sensitivity of the instrument.

Supplementary Materials

This PDF file includes:

Supplementary Text
Table S1
Figs. S1 to S7

REFERENCES AND NOTES

1. E. Quirico, L. V. Moroz, B. Schmitt, G. Arnold, M. Faure, P. Beck, L. Bonal, M. Ciarniello, F. Capaccioni, G. Filacchione, S. Erard, C. Leyrat, D. Bockelée-Morvan, A. Zinzi, E. Palomba, P. Drossart, F. Tosi, M. T. Capria, M. C. De Sanctis, A. Raponi, S. Fonti, F. Mancarella, V. Orofino, A. Barucci, M. I. Blecka, R. Carlson, D. Despan, A. Faure, S. Fornasier, M. S. Gudipati, A. Longobardo, K. Markus, V. Mennella, F. Merlin, G. Piccioni, B. Rousseau, F. Taylor, Refractory and semi-volatile organics at the surface of comet 67P/Churyumov-Gerasimenko: Insights from the VIRTIS/Rosetta imaging spectrometer. *Icarus* **272**, 32–47 (2016).
2. F. Capaccioni, A. Coradini, G. Filacchione, S. Erard, G. Arnold, P. Drossart, M. C. D. Sanctis, D. Bockelee-Morvan, M. T. Capria, F. Tosi, C. Leyrat, B. Schmitt, E. Quirico, P. Cerroni, V. Mennella, A. Raponi, M. Ciarniello, T. McCord, L. Moroz, E. Palomba, E. Ammannito, M. A. Barucci, G. Bellucci, J. Benkhoff, J. P. Bibring, A. Blanco, M. Blecka, R. Carlson, U. Carsenty, L. Colangeli, M. Combes, M. Combi, J. Crovisier, T. Encrenaz, C. Federico, U. Fink, S. Fonti, W. H. Ip, P. Irwin, R. Jaumann, E. Kuehrt, Y. Langevin, G. Magni, S. Mottola, V. Orofino, P. Palumbo, G. Piccioni, U. Schade, F. Taylor, D. Tiphene, G. P. Tozzi, P. Beck, N. Biver, L. Bonal, J.-P. Combe, D. Despan, E. Flamini, S. Fornasier, A. Frigeri, D. Grassi, M. Gudipati, A. Longobardo, K. Markus, F. Merlin, R. Orosei, G. Rinaldi, K. Stephan, M. Cartacci, A. Cicchetti, S. Giuppi, Y. Hello, F. Henry, S. Jacquinod, R. Noschese, G. Peter, R. Politi, J. M. Reess, A. Semery, The organic-rich surface of comet 67P/Churyumov-Gerasimenko as seen by VIRTIS/Rosetta. *Science* **347**, aaa0628 (2015).
3. L. Le Roy, K. Altwegg, H. Balsiger, J.-J. Berthelier, A. Bieler, C. Briois, U. Calmonte, M. R. Combi, J. De Keyser, F. Dhooghe, B. Fiethe, S. A. Fuselier, S. Gasc, T. I. Gombosi, M. Hässig, A. Jäckel, M. Rubin, C.-Y. Tzou, Inventory of the volatiles on comet 67P/Churyumov-Gerasimenko from Rosetta/ROSINA. *Astron. Astrophys.* **583**, A1 (2015).
4. I. P. Wright, S. Sheridan, S. J. Barber, G. H. Morgan, D. J. Andrews, A. D. Morse, CHO-bearing organic compounds at the surface of 67P/Churyumov-Gerasimenko revealed by Ptolemy. *Science* **349**, aab0673 (2015).
5. F. Goesmann, H. Rosenbauer, J. H. Bredehöft, M. Cabane, P. Ehrenfreund, T. Gautier, C. Giri, H. Krüger, L. L. Roy, A. J. MacDermott, S. McKenna-Lawlor, U. J. Meierhenrich, G. M. Muñoz Caro, F. Raulin, R. Roll, A. Steele, H. Steininger, R. Sternberg, C. Szopa, W. Thiemann, S. Ulamec, Organic compounds on comet 67P/Churyumov-Gerasimenko revealed by COSAC mass spectrometry. *Science* **349**, aab0689 (2015).
6. N. Hänni, K. Altwegg, M. Combi, S. A. Fuselier, J. De Keyser, M. Rubin, S. F. Wampfler, Identification and characterization of a new ensemble of cometary organic molecules. *Nat. Commun.* **13**, 3639 (2022).
7. K. Altwegg, H. Balsiger, N. Hänni, M. Rubin, M. Schuhmann, I. Schroeder, T. Sémon, S. Wampfler, J.-J. Berthelier, C. Briois, M. Combi, T. I. Gombosi, H. Cottin, J. De Keyser, F. Dhooghe, B. Fiethe, S. A. Fuselier, Evidence of ammonium salts in comet 67P as explanation for the nitrogen depletion in cometary comae. *Nat. Astron.* **4**, 533–540 (2020).
8. K. Altwegg, M. Combi, S. A. Fuselier, N. Hänni, J. De Keyser, A. Mahjoub, D. R. Müller, B. Pestoni, M. Rubin, S. F. Wampfler, Abundant ammonium hydrosulphide embedded in cometary dust grains. *Mon. Not. R. Astron. Soc.* **516**, 3900–3910 (2022).

9. E. F. van Dishoeck, G. A. Blake, Chemical evolution of star-forming regions. *Annu. Rev. Astron. Astrophys.* **36**, 317–368 (1998).
10. M. Rubin, K. Altwegg, H. Balsiger, J.-J. Berthelier, M. R. Combi, J. De Keyser, M. Drozdovskaya, B. Fiethe, S. A. Fuselier, S. Gasc, T. I. Gombosi, N. Hänni, K. C. Hansen, U. Mall, H. Rème, I. R. H. G. Schroeder, M. Schuhmann, T. Sémon, J. H. Waite, S. F. Wampfler, P. Wurz, Elemental and molecular abundances in comet 67P/Churyumov-Gerasimenko. *Mon. Not. R. Astron. Soc.* **489**, 594–607 (2019).
11. A. Mahjoub, M. J. Poston, K. P. Hand, M. E. Brown, R. Hodyss, J. Blacksberg, J. M. Eiler, R. W. Carlson, B. L. Ehlmann, M. Choukroun, Electron irradiation and thermal processing of mixed-ices of potential relevance to Jupiter Trojan asteroids. *Astrophys. J.* **820**, 141 (2016).
12. A. Mahjoub, M. J. Poston, J. Blacksberg, J. M. Eiler, M. E. Brown, B. L. Ehlmann, R. Hodyss, K. P. Hand, R. Carlson, M. Choukroun, Production of sulfur allotropes in electron irradiated Jupiter trojans ice analogs. *Astrophys. J.* **846**, 148 (2017).
13. M. J. Poston, A. Mahjoub, B. L. Ehlmann, J. Blacksberg, M. E. Brown, R. W. Carlson, J. M. Eiler, K. P. Hand, R. Hodyss, I. Wong, Visible near-infrared spectral evolution of irradiated mixed ices and application to kuiper belt objects and Jupiter trojans. *Astrophys. J.* **856**, 124 (2018).
14. A. Mahjoub, M. E. Brown, M. J. Poston, R. Hodyss, B. L. Ehlmann, J. Blacksberg, M. Choukroun, J. M. Eiler, K. P. Hand, Effect of H2S on the near-infrared spectrum of irradiation residue and applications to the kuiper belt object (486958) arrokoth. *Astrophys. J. Lett.* **914**, L31 (2021).
15. I. Wong, M. E. Brown, J. Blacksberg, B. L. Ehlmann, A. Mahjoub, Hubble ultraviolet spectroscopy of Jupiter trojans. *Astron. J.* **157**, 161 (2019).
16. E. T. Parker, H. J. Cleaves, J. P. Dworkin, D. P. Glavin, M. Callahan, A. Aubrey, A. Lazcano, J. L. Bada, Primordial synthesis of amines and amino acids in a 1958 Miller H2S-rich spark discharge experiment. *Proc. Natl. Acad. Sci. U.S.A.* **108**, 5526–5531 (2011).
17. H. Balsiger, K. Altwegg, P. Bochsler, P. Eberhardt, J. Fischer, S. Graf, A. Jäckel, E. Kopp, U. Langer, M. Mildner, J. Müller, T. Riesen, M. Rubin, S. Scherer, P. Wurz, S. Wüthrich, E. Arijs, S. Delanoye, J. D. Keyser, E. Neefs, D. Nevejans, H. Rème, C. Aoustin, C. Mazelle, J.-L. Médale, J. A. Sauvaud, J.-J. Berthelier, J.-L. Bertaux, L. Duvet, J.-M. Illiano, S. A. Fuselier, A. G. Ghielmetti, T. Magoncelli, E. G. Shelley, A. Korth, K. Heerlein, H. Lauche, S. Livi, A. Loose, U. Mall, B. Wilken, F. Gliem, B. Fiethe, T. I. Gombosi, B. Block, G. R. Carignan, L. A. Fisk, J. H. Waite, D. T. Young, H. Wollnik, Rosina – Rosetta orbiter spectrometer for ion and neutral analysis. *Space Sci. Rev.* **128**, 745–801 (2007).
18. K. Altwegg, H. Balsiger, J. J. Berthelier, A. Bieler, U. Calmonte, S. A. Fuselier, F. Goesmann, S. Gasc, T. I. Gombosi, L. Le Roy, J. de Keyser, A. Morse, M. Rubin, M. Schuhmann, M. G. G. T. Taylor, C.-Y. Tzou, I. Wright, Organics in comet 67P – a first comparative analysis of mass spectra from ROSINA–DFMS, COSAC and Ptolemy. *Mon. Not. R. Astron. Soc.* **469**, S130–S141 (2017).
19. U. Calmonte, K. Altwegg, H. Balsiger, J. J. Berthelier, A. Bieler, G. Cessateur, F. Dhooghe, E. F. van Dishoeck, B. Fiethe, S. A. Fuselier, S. Gasc, T. I. Gombosi, M. Hässig, L. Le Roy, M. Rubin, T. Sémon, C.-Y. Tzou, S. F. Wampfler, Sulphur-bearing species in the coma of comet 67P/Churyumov–Gerasimenko. *Mon. Not. R. Astron. Soc.* **462**, S253–S273 (2016).
20. U. Calmonte, K. Altwegg, H. Balsiger, J.-J. Berthelier, A. Bieler, J. De Keyser, B. Fiethe, S. A. Fuselier, S. Gasc, T. I. Gombosi, L. Le Roy, M. Rubin, T. Sémon, C.-Y. Tzou, S. F. Wampfler, Sulphur isotope mass-independent fractionation observed in comet 67P/Churyumov-–Gerasimenko by Rosetta/ROSINA. *Mon. Not. R. Astron. Soc.* **469**, S787–S803 (2017).
21. F. J. Ciesla, S. A. Sandford, Organic synthesis via irradiation and warming of ice grains in the solar nebula. *Science* **336**, 452–454 (2012).
22. J. A. Wood, Pressure and temperature profiles in the solar nebula. *Space Sci. Rev.* **92**, 87–93 (2000).
23. A. Jiménez-Escobar, G. M. Muñoz Caro, Y.-J. Chen, Sulphur depletion in dense clouds and circumstellar regions. Organic products made from UV photoprocessing of realistic ice analogs containing H2S. *Mon. Not. R. Astron. Soc.* **443**, 343–354 (2014).
24. A. Jiménez-Escobar, G. M. Muñoz Caro, A. Ciaravella, C. Cecchi-Pestellini, R. Candia, G. Micela, Soft X-ray irradiation of H_2S ice and the presence of S_2 in comets. *Astrophys. J. Lett.* **751**, L40 (2012).
25. M. Garozzo, D. Fulvio, Z. Kanuchova, M. E. Palumbo, G. Strazzulla, The fate of S-bearing species after ion irradiation of interstellar icy grain mantles. *Astron. Astrophys.* **509**, A67 (2010).
26. N. Fray, A. Bardyn, H. Cottin, K. Altwegg, D. Baklouti, C. Briois, L. Colangeli, C. Engrand, H. Fischer, A. Glasmachers, E. Grün, G. Haerendel, H. Henkel, H. Höfner, K. Hornung, E. K. Jessberger, A. Koch, H. Krüger, Y. Langevin, H. Lehto, K. Lehto, L. Le Roy, S. Merouane, P. Modica, F.-R. Orthous-Daunay, J. Paquette, F. Raulin, J. Rynö, R. Schulz, J. Silén, S. Siljeström, W. Steiger, O. Stenzel, T. Stephan, L. Thirkell, R. Thomas, K. Torkar, K. Varmuza, K.-P. Wanczek, B. Zaprudin, J. Kissel, M. Hilchenbach, High-molecular-weight organic matter in the particles of comet 67P/Churyumov–Gerasimenko. *Nature* **538**, 72–74 (2016).
27. J. A. Paquette, K. Hornung, O. J. Stenzel, J. Rynö, J. Silen, J. Kissel, M. Hilchenbach, The $^{34}S/^{32}S$ isotopic ratio measured in the dust of comet 67P/Churyumov-Gerasimenko by Rosetta/COSIMA. *Mon. Not. R. Astron. Soc.* **469**, S230–S237 (2017).
28. P. Klaboe, The vibrational spectra of 1,4-dithiane and 1,3,5-trithiane. *Spectrochim. Acta A* **25**, 1437–1447 (1969).
29. H. Wieser, P. J. Krueger, E. Muller, J. B. Hyne, Vibrational spectra and a force field for H2S3 and H2S4. *Can. J. Chem.* **47**, 1633–1637 (1969).
30. C. N. R. Rao, R. Venkataraghavan, T. R. Kasturi, Contribution to the infrared spectra of organosulphur compounds. *Can. J. Chem.* **42**, 36–42 (1964).
31. L. R. Peebles, P. Marshall, High-accuracy coupled-cluster computations of bond dissociation energies in SH, H2S, and H2O. *J. Chem. Phys.* **117**, 3132–3138 (2002).
32. A. Ruf, A. Bouquet, P. Boduch, P. Schmitt-Kopplin, V. Vinogradoff, F. Duvernay, R. G. Urso, R. Brunetto, L. Le Sergeant d'Hendecourt, O. Mousis, G. Danger, Organosulfur compounds formed by sulfur ion bombardment of astrophysical ice analogs: Implications for moons, comets, and kuiper belt objects. *Astrophys. J. Lett.* **885**, L40 (2019).
33. A. Ruf, A. Bouquet, P. Schmitt-Kopplin, P. Boduch, O. Mousis, G. Danger, Sulfur ion irradiation experiments simulating space weathering of solar system body surfaces. *Astron. Astrophys.* **655**, A74 (2021).
34. A. Tieftrunk, G. Pineau des Forets, P. Schilke, C. M. Walmsley, SO and H_2S in low density molecular clouds. *Astron. Astrophys.* **289**, 579–596 (1994).
35. D. P. Ruffle, T. W. Hartquist, P. Caselli, D. A. Williams, The sulphur depletion problem. *Mon. Not. R. Astron. Soc.* **306**, 691–695 (1999).
36. E. B. JENKINS, A unified representation of gas-phase element depletions in the interstellar medium. *Astrophys. J.* **700**, 1299–1348 (2009).
37. P. M. Woods, A. Occhiogrosso, S. Viti, Z. Kaňuchová, M. E. Palumbo, S. D. Price, A new study of an old sink of sulphur in hot molecular cores: The sulphur residue. *Mon. Not. R. Astron. Soc.* **450**, 1256–1267 (2015).
38. M. Kama, O. Shorttle, A. S. Jermyn, C. P. Folsom, K. Furuya, E. A. Bergin, C. Walsh, L. Keller, Abundant refractory sulfur in protoplanetary disks. *Astrophys. J.* **885**, 114 (2019).
39. H. Naraoka, Y. Takano, J. P. Dworkin, Y. Oba, K. Hamase, A. Furusho, N. O. Ogawa, M. Hashiguchi, K. Fukushima, D. Aoki, P. Schmitt-Kopplin, J. C. Aponte, E. T. Parker, D. P. Glavin, H. L. McLain, J. E. Elsila, H. V. Graham, J. M. Eiler, F.-R. Orthous-Daunay, C. Wolters, J. Isa, V. Vuitton, R. Thissen, S. Sakai, T. Yoshimura, T. Koga, N. Ohkouchi, Y. Chikaraishi, H. Sugahara, H. Mita, Y. Furukawa, N. Hertkorn, A. Ruf, H. Yurimoto, T. Nakamura, T. Noguchi, R. Okazaki, H. Yabuta, K. Sakamoto, S. Tachibana, H. C. Connolly, D. S. Lauretta, M. Abe, T. Yada, M. Nishimura, K. Yogata, A. Nakato, M. Yoshitake, A. Suzuki, A. Miyazaki, S. Furuya, K. Hatakeda, H. Soejima, Y. Hitomi, K. Kumagai, T. Usui, T. Hayashi, D. Yamamoto, R. Fukai, K. Kitazato, S. Sugita, N. Namiki, M. Arakawa, H. Ikeda, M. Ishiguro, N. Hirata, K. Wada, Y. Ishihara, R. Noguchi, T. Morota, N. Sakatani, K. Matsumoto, H. Senshu, R. Honda, E. Tatsumi, Y. Yokota, C. Honda, T. Michikami, M. Matsuoka, A. Miura, H. Noda, T. Yamada, K. Yoshihara, K. Kawahara, M. Ozaki, Y. Iijima, H. Yano, M. Hayakawa, T. Iwata, R. Tsukizaki, H. Sawada, S. Hosoda, K. Ogawa, C. Okamoto, N. Hirata, K. Shirai, Y. Shimaki, M. Yamada, T. Okada, Y. Yamamoto, H. Takeuchi, A. Fujii, Y. Takei, K. Yoshikawa, Y. Mimasu, G. Ono, N. Ogawa, S. Kikuchi, S. Nakazawa, F. Terui, S. Tanaka, T. Saiki, M. Yoshikawa, S. Watanabe, Y. Tsuda, Soluble organic molecules in samples of the carbonaceous asteroid (162173) Ryugu. *Science* **379**, eabn9033 (2023).
40. A. Zherebker, Y. Kostyukevich, D. S. Volkov, R. G. Chumakov, L. Friederici, C. P. Rüger, A. Kononikhin, O. Kharybin, A. Korochantsev, R. Zimmermann, I. V. Perminova, E. Nikolaev, Speciation of organosulfur compounds in carbonaceous chondrites. *Sci. Rep.* **11**, 7410 (2021).
41. L. R. Nittler, R. M. Stroud, J. M. Trigo-Rodríguez, B. T. De Gregorio, C. M. O. Alexander, J. Davidson, C. E. Moyano-Cambero, S. Tanbakouei, A cometary building block in a primitive asteroidal meteorite. *Nat. Astron.* **3**, 659–666 (2019).
42. L. G. Vacher, R. C. Ogliore, C. Jones, N. Liu, D. A. Fike, Cosmic symplectite recorded irradiation by nearby massive stars in the solar system's parent molecular cloud. *Geochim. Cosmochim. Acta* **309**, 135–150 (2021).
43. S. N. Milam, J. A. Stansberry, G. Sonneborn, C. Thomas, The *James Webb Space Telescope*'s plan for operations and instrument capabilities for observations in the solar system. *Publ. Astron. Soc. Pac.* **128**, 018001 (2016).
44. M. S. P. Kelley, C. E. Woodward, D. Bodewits, T. L. Farnham, M. S. Gudipati, D. E. Harker, D. C. Hines, M. M. Knight, L. Kolokolova, A. Li, I. de Pater, S. Protopapa, R. W. Russell, M. L. Sitko, D. H. Wooden, Cometary Science with the *James Webb Space Telescope*. *Publ. Astron. Soc. Pac.* **128**, 018009 (2016).
45. A. S. Rivkin, F. Marchis, J. A. Stansberry, D. Takir, C. Thomas, Asteroids and the *James Webb Space Telescope*. *Publ. Astron. Soc. Pac.* **128**, 018003 (2016).
46. I. Wong, M. E. Brown, A hypothesis for the color bimodality of Jupiter trojans. *Astron. J.* **152**, 90 (2016).
47. K. P. Hand, R. W. Carlson, H2O2 production by high-energy electrons on icy satellites as a function of surface temperature and electron flux. *Icarus* **215**, 226–233 (2011).
48. C. J. Bennett, C. Pirim, T. M. Orlando, Space-weathering of solar system bodies: A laboratory perspective. *Chem. Rev.* **113**, 9086–9150 (2013).

49. A. G. Yeghikyan, Irradiation of dust in molecular clouds. II. Doses produced by cosmic rays. *Astrophysics* **54**, 87–99 (2011).

Acknowledgments: This work has been conducted at the JPL, Caltech, under a contract with the National Aeronautics and Space Administration (NASA), and at the Caltech Division of Geological and Planetary Sciences. ROSINA would not have produced such outstanding results without the work of the many engineers, technicians, and scientists involved in the mission, in the Rosetta spacecraft team, and in the ROSINA instrument team over the past 20 years, whose contributions are acknowledged. Rosetta is an ESA mission with contributions from its member states and NASA. We acknowledge herewith the work of the whole ESA Rosetta team. We would like to thank anonymous reviewers for valuable comments. **Funding:** This work has been supported in part by the NASA/RDAP program (80NM0018F0612) and by the Keck Institute for Space Studies (KISS). Part of this work was supported by NASA/DDAP program under grant no. 80NSSC21K1015. **Author contributions:** A.M. wrote the manuscript. A.M. and M.J.P. led the work on laboratory simulations and analyzed the data from laboratory measurements. K.A., M.R., and N.H. analyzed the data from ROSINA-DFMS measurements. K.P.H. built and developed the experimental setup used on laboratory simulations and supervised the experimental work. M.E.B., J.M.E., and J.B. supervised the work. B.L.E., R.H., and J.B. participated in the laboratory work. All authors participated in the interpretation of the results and read and commented on the manuscript. **Competing interests:** The authors declare that they have no competing interests. **Data and materials availability:** The datasets analyzed during the current study together with a user manual for data analysis are available in the ESA-PSA archive (www.cosmos.esa.int/web/psa/rosetta) or the NASA PDS archive (https://pdssbn.astro.umd.edu/data_sb/missions/rosetta/index.html). Laboratory simulations data are available at Dryad (https://datadryad.org/stash/share/q3OXw5x2Xlgze7zZ_ss8_-U54pUOzzZFttVrpm8gUzo). All data needed to evaluate the conclusions in the paper are present in the paper and/or the Supplementary Materials.

Submitted 7 February 2023
Accepted 1 May 2023
Published 7 June 2023
10.1126/sciadv.adh0394